ANALYZE OF WELDING REGIME IN LASER WELDING WITH FULL FACTORIAL DESIGN EXPERIMENTS

Remus Boboescu[1] Ramona Laslău[2]
1 University Romania remus_boboescu@yahoo.com
2 University Polithenica Timisoara Polithenica Timisoara Romania ramonalaslau@yahoo.com

ABSTRACT:.For keyhole welding regime there is a particular of the weld cross-section shape aspect given by the heat affected zone area. It analyzes the laser welds made with Nd:YAG laser on low alloy steel plates using irradiation in continuously regime. The power, welding speed and defocusing are varied. Experiments were conducted after the full factorial experimental design 2^2. This showed the effect of laser power for setting keyhole welding regime
KEY WORDS: laser keyhole welding, full factorial design, laser beam defocusing, heat affected zone.

1. INTRODUCTION

Laser welding has two distinct regimes of conduction welding and keyhole welding regime which differ in the weld penetration and weld cross section shape. Keyhole phenomenon causes separation between the situations where laser welding is performed. This defines two regimes of welding: conduction welding and keyhole welding regime. Investigation and study of laser welding process has two main directions. These are investigations of the welding process (on-line) and investigations of made welds (off-line). In this second category were classified experimental investigations carried out in the paper.

Studies during the welding process refers to the investigation of the weld pool surface and oscillations that occur in this using, X-ray images, fast shooting, spectral analysis of the radiation emitted from laser- material interaction zone, analysis of the radiation emitted from welding bath using photodiodes with an absorption in the UV and IR, analysis of sounds emitted during welding and the variation of radiation intensity reflected the weld surface by a control source (He-Ne laser or laser diode) using a photo detector. These studies aim to study the weld pool and keyhole as main problems and less to study the parameters that control the welding process.

Weld analysis studies weld cross section shape, weld heat affected zone size, presence of porosity in the weld and metallographic appearance of the weld and strength tests on welded joints. Other aspects of are related to the weld surface through its roughness and solid waves (waves on the surface of the weld).

Investigation of welds and welding process is accompanied by modeling to knowledge and predict the welding process. Is proposed a separation between analytical modeling for that is important phenomenological component and experimental modeling that ignores phenomenological aspect. Using numerical modeling and numerical methods are considered as an additional instrument for analytical modeling. The difference between the analytical models is due by proposed simplifying assumptions. It proposes a gradual approach them. This is considered a heat source to the material surface identified by the laser beam, and then considers moving heat source feature of laser machining processes. Melt production occurs in a specific form which requires the distribution of heat flux density initially considered. It comes to complex models that consider a conical, cylindrical or hemispherical keyhole [1] [2] [3] [4]. Experimental modeling make a link between the parameters controlling the welding process (called factors of influence) and sizes measured or calculated (called objective function). This connection is due by correlation functions (equations) called mathematical or empirical models. Experimental modeling used factorial experimental plans which vary several factors simultaneously. Related to this question is the choice of type of mathematical formula (polynomial, logarithmic) that describes the type of variation and the creation of a statistical study of variation. It notes using quadratic formula (second-degree polynomials) and use the method of variation analysis ANOVA.

Conduction welding regime. This regime is called conduction limited welding. The solid-liquid interface heat transfer mechanism is exclusively by conduction. Heat is conducted directly from the heat source that occurs due laser radiation from the workpiece surface within the material. Conduction welding regime is characterized by irradiation sufficient to produce piece surface melting and vaporization but not enough to produce vaporization in the depth of material. For conduction welding regime values of F ratio between the weld width and weld depth are higher than 1, $F \geq 1$. As an indicative value for the weld depth in conduction regime is 1.5 mm [5]. Defects that are obtained in conduction welding regime are cracks on the weld surface.

Keyhole welding regime. This welding regime involves the keyhole phenomenon in weld pool which involves the values of laser beam intensities that exceed threshold needed to produce a vapor front propagation in the material. Heat transfer mechanism at solid-liquid interface involves both conduction and convection due to the melt movement in the weld pool. In weld cross section there is a welding defects gas bubbles, the presence of this pore led to the designation of keyhole regime ("key hole"). F ratio between weld width and weld depth has a smaller value than 1, $F \leq 1$. Defects in welds are obtained for the keyhole welding regime are gas porosity due to dissolution into the melt a gas bubbles and vacuum large areas. The presence of the Keyhole and vapor within the material made pushing melting front (solid-liquid interface) inside the material. This provides increased weld penetration. For welds made in experiments the two welding regimes are shown in Figure 1 by the weld cross section.

Figure 1. Image of weld cross-section of the weld a) weld in the conduction regime b)weld in keyhole regime

Getting the melt within the material is given by the laser beam intensity on workpiece surface and the interaction time between laser radiation and material. Range of values for these parameters for our experiments is: the laser beam intensity 0.54×10^5 -10.61×10^5 W/cm^2 and interaction time 24-480 ms. Varied parameters laser beam power, welding speed and defocus have the following effects on laser beam intensity and interaction time:

- Power. Laser beam intensity increases with power. The amount of melt increases with laser beam intensity. From a certain value, intensity too high not favors material melting, favors its vaporization.

-Welding speed. Increasing welding speed decreases the interaction time between laser radiation and material. As the interaction time is less, the melted zone dimensions are smaller.

- Defocus. Defocus, by lowering the focal plane inside piece produce a decrease in intensity at the workpiece surface by increasing laser beam spot on the workpiece surface. This will increase the interaction time between laser and material. Focusing within the piece associated with the presence of keyhole in welding bath will spread the radiation into keyhole and increase coupling of laser radiation and material. Defocus can have such different effects on the material melting. You can not preset a clear trend of increase or decrease the melted area with defocus. From this point of view is necessary to analyze the effects of defocus on the geometric characteristics of the weld.

Studies for laser welding of various metals pursue knowledge and optimizing the welding process and also to show structural changes that occur in the metal after laser beam irradiation. Thus laser welding of steels is presented in [6], [7],[8] Laser welding of aluminum alloys has been presented in the works [9], [10]. Welding of titanium alloys were presented in [11] Laser welding of nickel alloys are presented in [12] and [13]. Study of laser welding process for nickel alloys has been presented in [14], [15].

The paper proposes the identification and use of quantities that can characterize welds under keyhole welding regime. It looks like those in characterizing keyhole regime occurs sizes associated with both weld cross section and weld surface. Experimental factorial design 2^2 used presents for higher levels of power keyhole welding regime and for the lower power level presents the conduction welding regime. It will discuss variation of the response functions relative to varied parameters power and welding speed.

2. EXPERIMENTS

The experiment consisted in made lines of fusion (welds), 110 mm long, on Dillimax 500 steel plates with thickness of 10 mm (carbon steel, carbon content ≤ 0.16 %). Was used a Nd: YAG Trumph Haas 3006D laser source with 3kW maximum power on a continuous wave regime CW. Laser beam was transmitted through a optical fiber with core diameter of 0.6 mm. The focus system made a focal spot with 0.6 mm diameter. Lens focal length was 200 mm. As protective gas argon was used with a flow rate of 20 l/min. Parameters varied in the experiments are presented in Figure 2.

In experiments was varied the laser power, welding speed and distance between focal plane and piece surface (defocusing or defocusing depth) figure 2. Welds were cut in the stable part of the weld near the place where welding process was stopped. Weld section was processed metallographic. Weld width, near the piece surface, and weld depth were examined using a microscope with precision of 0.01 mm. Melted area was measured directly by its footprint**.** Defocusing values are considered negative if the laser beam focus inside the piece**.**

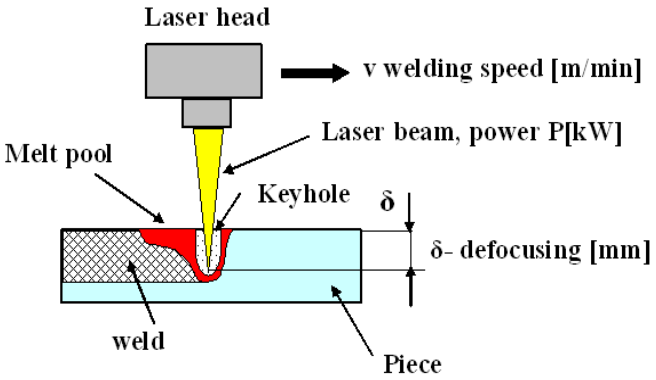

Figure 2. Scheme of keyhole welding pool with varied parameters in welding process

In the experiments were varied power and welding speed. To statistically analyze the effects of parameters was necessary to introduce a dimensionless parameter values. Transformations between the two systems of parameters values (actual values and coded values) are based by following relationships:

$$A = P - 2 \text{ [-]} \quad (1)$$

$$B = -2.33 + 2.22v \text{ [-]} \quad (2)$$

The experimental plan is presented in Table 1 with actual values that coded for power and cutting speed.

Table 1. Varied parameters values in experiment

	power		speed	
weld	A[-]	P[kW]	B [-]	v[m/min]
1	-1	1	-1	0.6
2	+1	3	-1	0.6
3	-1	1	+1	1.5
4	+1	3	+1	1.5
5	0	2	0	1
6	0	2	0	1

Analysis procedure consisted of presenting the results of the mathematical model, ANOVA table showing the correlation coefficients associated with the mathematical model, Pareto chart showing the hierarchy of effects and response surface is a graphic representation of mathematical model. For the mathematical model were presented two forms for real values laser power and welding speed and for coded system values. The first allows rapid application of formulas and the second allows direct analysis of the values of regression coefficients. Based on these values were achieved Pareto charts.Figure 3 shows the analysis weld scheme and analyzed sizes that characterizing the weld.

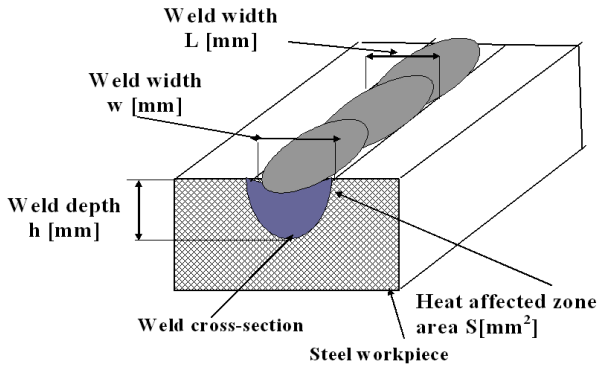

Figure 3. Scheme of weld with measured sizes

The paper analyzed variations the following sizes: weld width, shape ratio of weld cross section and the heat affected zone area on the weld cross section.

Weld width L [mm] was obtained as a result of three measurements on the weld surface at the beginning, middle and end of the welding process.The weld width characterized in general the weld and it is independent of the area in this cross section in weld was performed.

F ratio (w/h) is the ratio beetwen weld width and weld depth on the weld cross section.This ratiois associated with the welding regime characterization.Values of F ratio below unity shows keyhole welding regime.

A heat affected zone area S[mm^2] was measured on the weld cross section. It is given by the isothermal line of transformation metal structure which is well below the melting temperature. Area heat affected zone containing molten zone area. Heat affected area can be measured with greater accuracy than the area of molten zone.

3. WELD WIDTH

The mathematical model for weld width at defocusing $\delta = 0$ is given by relations (3) and (4). Statistical analysis by ANOVA method is given in Table 2.

$$L = 2.08866 + 0.29\,A - 0.375\,B \quad (3)$$

$$L = 0.63285 + 0.29P - 0.8325v \quad (4)$$

Table 2. ANOVA table for weld width L at $\delta = 0$

Effect	Sum of Squares	DF	Mean. Sq.	f-Ratio	P-val
A(power)	0.336	1	0.336	1.80	0.27
B(speed)	0.562	1	0.562	3.01	0.18
Total error	0.561	3	0.187		
Total (corr.)	1.460	5			
$R^2 = 0.61$			$R^2(adj.for\ d.f) = 0.35$		

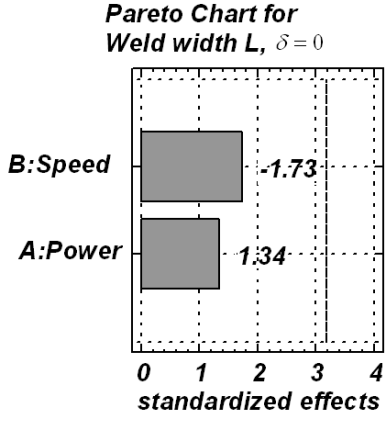

Figure 4. Pareto Chart for weld width at $\delta = 0$

In figure 4 is presented Pareto chart to weld width for the laser beam focus to the workpiece surface. It is noted that the weld width with increases with power and decreases with welding speed. Effect of welding speed is close to that of power and is height than this. The two parameters effects were not statistically significant. Weld width was measured considering the entire weld. It shows that in this case the weld width presents dynamic phenomena occurring in the welding pool. Melt movement produces increased role of welding speed and produces oscillations between power and welding speed as the first effect.

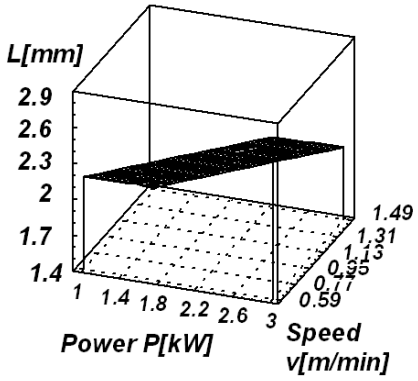

Figure 5. Response surface for weld width at $\delta = 0$

Response surface in Figure 5 shows that the experimental weld width increases with power and decreases with welding speed. It is recommended the high values for weld width but not the highest.

The mathematical model for weld width at defocusing $\delta = -2mm$ is given by equations (5) and (6). The correlation coefficients for the mathematical model associated with the mathematical and statistical method of ANOVA analysis of variances are given by equations (7) and (8).

$$L = 2.0966 + 0.875A - 0.545B \quad (5)$$

$$L = 1.61645 + 0.875A - 1.20990v \quad (6)$$

$$R^2 = 0.86 \quad (7)$$

$$R^2(adj.for\ d.f) = 0.77 \quad (8)$$

Figure 6 presents the Pareto chart for the weld width where the laser beam was focused within the piece. It shows that the weld width increases with power and decreases with welding speed. The first effect is that of power. This is statistically significant. It shows that in this case the welding process is more stable than when the laser beam focus at the workpiece surface. Even if the influence of welding speed is high the first effect is that of power.

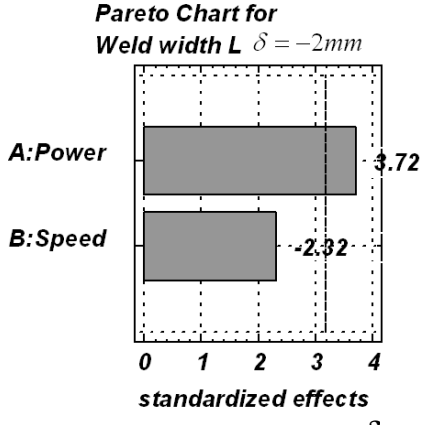

Figure 6. Pareto Chart for weld width at $\delta = -2mm$

Response surface from figure 7 shows that the on the experimental weld width increases with power. Variation of the weld width with welding speed is reduced. Maximum values for the weld width is obtained at maximum power and minimum welding speed. It is noted that for the focus inside piece weld width is higher than for the focus to the workpiece surface. This is explained by increasing the laser beam spot size at the workpiece surface for the laser beam focus within the piece.

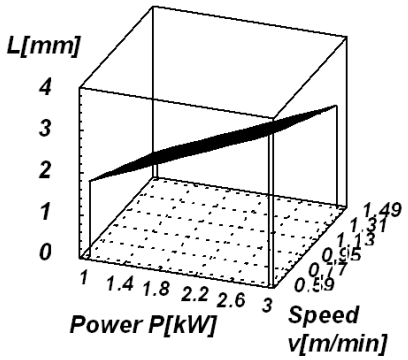

Figure 7. Response surface for weld width at $\delta = -2mm$

4. RATIO F

The mathematical model for the ratio F at defocusing $\delta = 0$ is given by equations (9) and (10). Study of variation by the ANOVA method is presented in Table 3.

$$F = 1.535 - 1.025A + 0.375B \quad (9)$$

$$F = 4.45875 - 1.025P + 0.8325v \quad (10)$$

Figure 8 shows the Pareto chart for the ratio F to focus the laser beam to the workpiece surface. It shows that ratio F decreases with power and increases with welding speed.

Table 3. ANOVA table for Ratio F at $\delta = 0$

Effect	Sum of Squares	DF	Mean. Sq.	f-Ratio	P-val
A(power)	4.202	1	4.202	8.81	0.05
B(speed)	0.562	1	0.562	1.18	0.35
Total error	1.431	3	0.477		
Total (corr.)	6.196	5			
$R^2 = 0.768$ $R^2(adj.for\,d.f.) = 0.614$					

As the decreasing ratio F takes place transition from conduction welding regime to keyhole welding regime. Welding speed has a relatively height contribution in comparison with that of power. Presented effects are not statistically significant. This is due to the instability of the welding process.

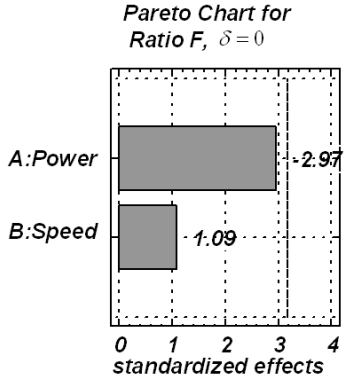

Figure 8. Pareto Chart for ratio F at $\delta = 0$

Response surface in Figure 9 shows that on the experimental field is a decrease in ratio F. Minimum values of F ratio are obtained at maximum power and minimum welding speed

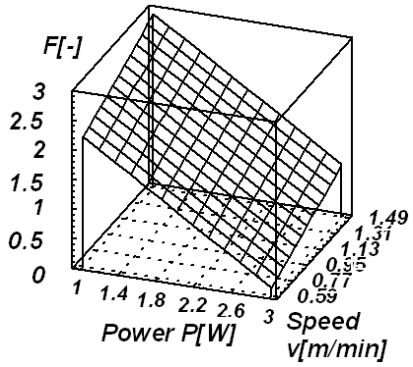

Figure 9. Response surface for Ratio F at $\delta = 0$

To obtain the welding procedure Keyhole F ratio values need to be below unit 1. Minimum values of F ratio were associated with the presence of many pores in the weld. This is known as a strong Keyhole welding regime. Maximum values F ratio show conduction welding regime for which there is not of the weld in material. There is only melting the material at surface.

The mathematical model for the ratio F at defocusing $\delta = -2mm$ is given by equations (11) and (12). Study the variations by ANOVA method is presented in Table 4.

$$F = 1.71 - 1.0925A - 0.2425B \quad (11)$$

$$F = 4.46 - 1.0925P - 0.53835v \quad (12)$$

Figure 10 shows the Pareto chart for the ratio F on the laser beam focus within the piece. F ratio decreases with power and decreases with welding speed. The main effect belongs of power. Note that in this case increases the role of power in comparison with the situation which focuses the laser beam was made at the workpiece surface.

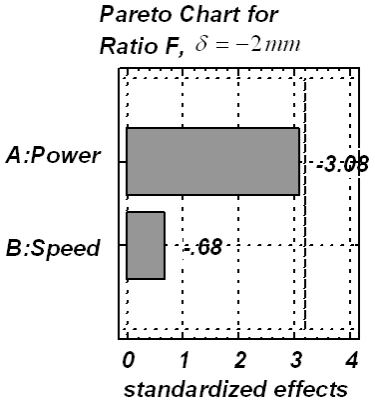

Figure 10. Pareto Chart for Ratio F at $\delta = -2mm$

Table 4. ANOVA table for Ratio F (w/h)at $\delta = -2mm$

Effect	Sum of Squares	DF	Mean. Sq.	f-Ratio	P-val
A(power)	4.774	1	4.774	9.47	0.5
B(speed)	0.235	1	0.235	0.47	0.55
Total error	1.512	3	0.504		
Total (corr)	6.521	5			
$R^2 = 0.76$ $R^2(adj.for\,d.f.) = 0.61$					

Effect of power is close to statistical significance. Low intensity of laser beam to the workpiece surface produces that in this case the setting of ratio F the welding regime to depend only by power. The negative sign associated with effect of

welding speed indicates in a certain measure the reducing of time of interaction between laser radiation and material favors melting front propagation material.

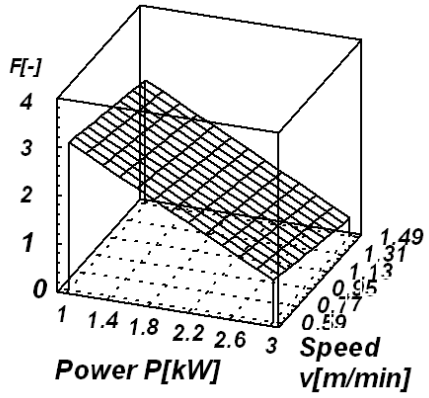

Figure 11. Response surface for Ratio F at $\delta = -2mm$

Response surface in Figure 11 shows that on the experimental F ratio values decrease with power. Minimum values for ratio F are obtained at maximum power.Note that minimum values can be obtained for the ratio F are higher than those obtained with laser beam focus at the workpiece surface.

5. HEAT AFFECTED ZONE AREA ON THE WELD CROSS SECTION

The mathematical model for heat affected zone area on weld cross section at defocusing is given by equations (13) and (14). ANOVA statistical analysis method is presented in Table 5.

$$S = 9.25 + 6.875A - 3.875B \quad (13)$$

$$S = -13.52875 + 6.875P - 8.6025v \quad (14)$$

E=mc^2

Table 5. ANOVA table for HAZ area S at $\delta = 0$

Effect	Sum of Squares	DF	Mean. Sq.	f-Ratio	P-val
A(power)	189.062	1	189.062	11.63	0.04
B(speed)	60.062	1	60.062	3.70	0.15
Total error	48.750	3	16.25		
Total (corr.)	297.875	5			
$R^2 = 0.83$			$R^2(adj.for\ d.f.) = 0.72$		

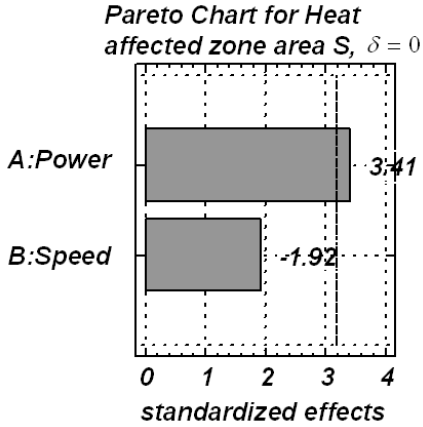

Figure 12. Pareto Chart for HAZ area at $\delta = 0$

Figure 12 shows the Pareto chart for the heat affected zone area to focus the laser beam to the workpiece surface. It is noted that the area of heat affected zone increases with power and decreases with welding speed. The main effect is the power that is statistically significant.

Response surface in Figure 13 shows that on the field of experimental heat affected zone area increases with power. Decrease the heat affected zone area is stronger at low welding speeds.

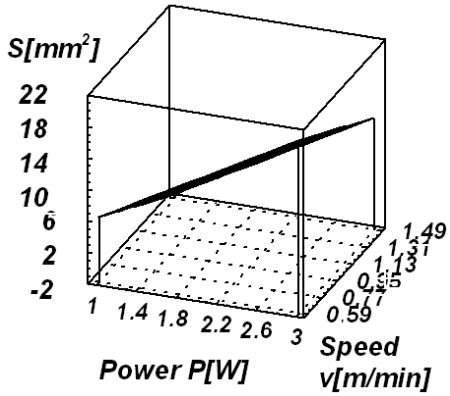

Figure 13. Response surface for HAZ area at $\delta = 0$

The mathematical model for heat affected zone area on the weld cross section at defocusing $\delta = -2mm$ is given by equations (15) and (16). ANOVA statistical analysis method is presented in Table 6.

$$S = 9.4166 + 8.125A - 3.875B \quad (15)$$

$$S = 2.19535 + 8.125P - 8.6025v \quad (16)$$

Table 6. ANOVA table for HAZ area S at $\delta = -2mm$

Effect	Sum of Squares	DF	Mean. Sq.	f-Ratio	P-val
A(power)	264.062	1	264.062	20.27	0.02
B(speed)	60.062	1	60.062	4.61	0.12
Total error	39.083	3	13.027		
Total (corr.)	363.208	5			
$R^2 = 0.89$			$R^2(adj.for\ d.f.) = 0.82$		

Figure 14 presents Pareto chart for the heat affected zone area where the laser beam focused within the piece. It is noted that the area of heat affected zone increases with power and decreases with welding speed. Power effect is statistically significant. Compared with case where the laser beam was focused on the workpiece surface effect speed decreased.

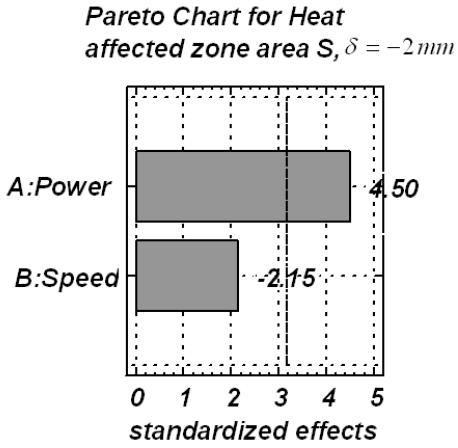

Figure 14. Pareto Chart for HAZ area at $\delta = -2mm$

Response surface in Figure 15 show that the heat affected zone area values increase with power. Variation shown is close to where the laser beam focusing is achieved at the workpiece surface. Area heat affected zone is a magnitude more sensitive to changes in power and welding speed values than the melted area. From analysis of the two situations is observed that the effect of defocus on the heat affected zone area is reduced.

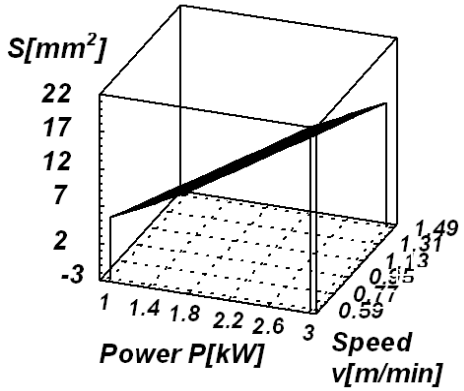

Figure 15. Response surface for HAZ area at $\delta = -2mm$

6. CONCLUSIONS

The paper also analyzes the effect of defocus on the welding process. We analyzed the variation of the three sizes that show the effect of radiation on the material. Weld width showes material melting at the workpiece surface. Heat affected zone area shows the effect of melting and heat transmission in material.The ratio F shows obtained welding regime, conduction regime or keyhole regime.

Correlated analysis of the three sizes can lead to the establishment of welding regime and estimate the amount of melt produced. They stated the following:

- Establish the welding regime depends on laser power.

- The amount of melt produced increases with power and decreases with welding speed.

- To focus the laser beam inside piese to increase the laser beam power effect the sizes analyzed.

The main results showed the experimental research related to use of a laser beam focus within the piece. In this situation welding process becomes more stable. Stability is manifests itself by maintaining a constant weld size along of weld and by reducing the number of pores in the weld.

7. REFERENCES

1. Ho Wen, Distribution of intensity absorbed by the keyhole wall in laser processing, *Proceedings of the International Conference, Applications of Lasers and Electro-Optics* (2004).
2. Xiangzhong Jin, Lijun Li, Yi Zhang, A study on fresnel absorption and reflections in the keyhole in deep penetration laser welding, *J. Phys. D: Appl. Phys*. Vol.35 pp:2304–2310 (2002).
3. Xiangzhong Jin, A three-dimensional model of multiple reflections for high-speed deep penetration laser welding an actual keyhole, *Optics and Lasers in Engineering* Vol.46 pp:83–93 (2008).
4. J. M. Jouvard, K Girard, O.Perret, Keyhole formation and power deposition in Nd:YAG laser spot welding, *J. Phys. D: Appl. Phys.*Vol. 34 pp:2894–2901 (2001)
5. Alexander F. H. Kaplan, Keyhole Laser Spot Welding, *Proceedings of the International Conference, Applications of Lasers and Electro-Optics* (2002)
6. M. Schmidt, A. Otto, C. Kageler, Analysis of YAG laser lap-welding of zinc coated steel sheets, *CIRP Annals - Manufacturing Technology* Vol.57 pp:213–216 (2008).
7. Jose Roberto Berretta, Wagner de Rossi, Maurıcio David Martins das Neves, Ivan Alves de Almeida, Nilson Dias Vieira Junior Pulsed Nd:YAG laser welding of AISI 304 to AISI 420 stainless steels, *Optics and Lasers in Engineering* Vol.45 pp:960–966, (2007).
8. Danny Ping, Pal Molian Q-switch N:YAG laser welding of AISI 304 stainless steel foils *Technical note Materials Science and Engineering A* Vol.486 pp.680–685 (2008)
9. A. Haboudou, P.Peyre, A.B.Vannes, G.Peix, Reduction of porosity content generated during Nd:YAG laser welding of A356 and AA5083 aluminium alloys, *Materials Science and Engineering A363* pp:40–52(2003).
10. Geoff J Shannon, *Spot and seam welding applications using Nd:YAG lasers,* Presentation at Unitek Miyachi Corporation.
11. E. Akman, A. Demir, T. Canel, T. Sınmazcelik, Laser welding of Ti6Al4V titanium alloys, *Journal of materials processing technology* Vol. 209 pp:3705–3713(2009).
12. A. Ancona, P.M. Lugara, D.Sorgente, L.Tricarico, Mechanical characterization of CO_2 laser beam butt welds of AA5083, *Journal of Materials Processing Technology* Vol.191 p:381–384 (2007).
13. K.H.. Leong and H. K. Geyer, Laser Beam Welding of Any Metal, *Proceedings of the International Conference, Applications of Lasers and Electro-Optics* (1998)
14. PA. Cantello , G. Ricciardi ,S. L. Gobbi, Laser Welding of Superalloys for the Manufacturing of Aeroengine Components *Annals of the ClRP* Vol. 45/ 1/1996.
15. W.J.Han, J.G.Byeon, K.S. Park, Welding characteristics of the Inconel plate using a pulsed Nd:YAG laser beam, *Journal of Materials Processing Technology* Vol.113 pp:234-236 (2001).